X-621-73-188
PREPRINT

ELECTROSTATIC VELOCITY-SPACE INSTABILITIES STIMULATED NEAR THE HARMONICS OF THE ELECTRON CYCLOTRON FREQUENCY IN THE IONOSPHERE

ROBERT F. BENSON

OCTOBER 1973

GSFC — GODDARD SPACE FLIGHT CENTER —
GREENBELT, MARYLAND

X-621-73-188
Preprint

ELECTROSTATIC VELOCITY-SPACE INSTABILITIES STIMULATED NEAR THE HARMONICS OF THE ELECTRON CYCLOTRON FREQUENCY IN THE IONOSPHERE

Robert F. Benson

Laboratory for Planetary Atmospheres

NASA — Goddard Space Flight Center

Greenbelt, Maryland 20771

October 1973

GODDARD SPACE FLIGHT CENTER

Greenbelt, Maryland

ABSTRACT

Satellite soundings of the topside ionosphere reveal diffuse signals on the low frequency side of nf_H when $nf_H < f_T$ where n is an integer and f_H and f_T are the electron cyclotron and upper hybrid frequencies, respectively. They extend no further than the mid-way point between $(n - 1)f_H$ and nf_H. The present observing conditions allow detection up to n = 10. The origin of the signals is attributed to the Harris instability of longitudinal plasma waves when $T_\perp / T_\parallel > 2n$ where $T_\perp$ and $T_\parallel$ refer to the temperature corresponding to the electron motion perpendicular and parallel to the earth's magnetic field, respectively. The large anisotropies are caused by collisionless cyclotron damping of energy from the high power sounder pulse. This energy is absorbed in a region which extends radially from the antenna a distance which is small compared to the antenna length but large compared to the antenna sheath region.

ELECTROSTATIC VELOCITY-SPACE INSTABILITIES STIMULATED NEAR THE HARMONICS OF THE ELECTRON CYCLOTRON FREQUENCY IN THE IONOSPHERE

INTRODUCTION

In 1959 Harris showed that obliquely traveling plasma waves, consisting of longitudinal oscillations of electrons, can be unstable in the presence of an anisotropic electron velocity distribution[1]. These instabilities occur near the harmonics of the electron cyclotron frequency f_H. This work has been extended to include ion motions with the result that instabilities are predicted at harmonics of the ion cyclotron frequency[2,3]. The theory has been related to plasma confinement experiments that produce large anisotropies in the ion velocity distribution in an attempt to explain the enhanced radiation often observed at these frequencies[4]. It is often difficult to interpret laboratory observations in terms of a single instability mechanism; the intense microwave radiation observed at nf_H (n = 1 to 19) by Wharton et al[5] is a case in point. It has been suggested that many of the laboratory observations may be explained in terms of a double distribution, i.e., where a hot anisotropic component of ions (or electrons) are superimposed on a cooler nearly isotropic component of the same species[6]. This interpretation has been used by Schwartz and Lichtenberg[7] to explain their observations related to velocity-space instabilities at nf_H with n = 1, 2, and 3. The present paper will present observations in the ionospheric plasma which

provide evidence for the stimulation of Harris-type instabilities at nf_H in a single electron distribution.

The original work of Harris[1] assumed $T_\perp/T_\parallel = \infty$ where $T_\perp$ is the temperature corresponding to electron motion perpendicular to the earth's magnetic field vector $\vec{B}$ and $T_\parallel$ is the temperature corresponding to electron motion parallel to $\vec{B}$. When finite $T_\perp/T_\parallel$ values are considered, the instability region extends below the nf_H value to a point midway between nf_H and $(n - 1)f_H$ for short wavelengths[8,9]. From the work of Gruber et al.[10] and Oya[11] it can be seen that the growth rate of the instability increases as the wavelength decreases; this behavior is illustrated schematically in Fig. 1 where the normalized dispersion curves are presented (the wave number being normalized by the inverse of the electron cyclotron radius R). Thus the Harris type instability is excited most readily when the frequency is near the mid point between the harmonics of nf_H. Also illustrated in Fig. 1 is the change in shape of the dispersion curve for a given nf_H as the upper hybrid frequency f_T crosses the nf_H value. It is evident from the figure that the instability can exist near nf_H only when $f_T > nf_H$.

OBSERVATIONS

The observations are from the ISIS 1 satellite. ISIS 1 is the third of 4 satellites of the series designated as International Satellites for Ionospheric Studies (the other three are Alouette 1, Alouette 2, and ISIS 2). Each satellite contains a sweep frequency rf sounder in order to obtain electron density vs. altitude profiles in the topside ionosphere, i.e., the region above the electron

density maximum near 300 km. The later satellites contain additional radio experiments, probes, particle detectors, and optical experiments and have evolved into extremely sophisticated ionospheric laboratories.[12] Of particular interest to the present study is the sounder experiment because, in addition to the electromagnetic waves used to obtain the electron density profiles, it generates plasma waves of low group velocity at fundamental frequencies in the ambient plasma. These received waves have been described as "resonances" because they appear as long duration signals (many milliseconds) which are received immediately after the transmission of a short (100 μ sec) rf pulse. An example of a swept-frequency recording (called an ionogram) that clearly illustrates these resonances is presented in Fig. 2 . An ionogram is composed of a large number of individual vertical scan lines, each at a separate frequency. Resonances are observed at the electron plasma frequency f_N, the upper hybrid frequency f_T, and at nf_H ($n = 1, 2, 3 \cdots$) where, using the conventional notation from the ionosphere literature, $f_N(\text{kHz}) \approx 9\ [N(\text{cm}^{-3})]^{1/2}$, $f_H(\text{kHz}) \approx (1/36)\ B(\gamma)$, $f_T^2 = f_N^2 + f_H^2$, and N and B are the ambient values for the electron density and magnetic field strength respectively ($1\gamma = 10^{-5}$ Gauss). The resonances at f_N and f_T have been interpreted in terms of the reception of obliquely traveling plasma waves of low group velocity which return to the sounder because of the local gradient of N, as first proposed by McAfee[13]; the theory has received considerable observational support[14]. Andrews and Fang[15] suggested that the same oblique echo mechanism may also be applied to the nf_H resonances ($n > 1$) whereas the ray tracing calculations of Muldrew[16] indicate that the gradient of f_N is of secondary importance compared with the gradient of f_H for these resonances.

The approach of Muldrew may account for the long durations observed with the low order harmonics of f_H but such propagation effects may not be as important for the higher order harmonics.[17] Also shown on Fig. 2 are resonances labeled f_{D1}, f_{Q3}, and f_{Q5}. These resonances are members of sequences of resonances that appear between the harmonics of f_H; the f_Q series[18] is observed above f_T and the f_D series[19] is observed below f_T. The f_Q resonances have been interpreted in terms of stimulated plasma waves with group velocities that are very nearly equal to the satellite velocity,[20] whereas the f_D resonances involve plasma waves with group velocities approximately an order of magnitude larger than the satellite velocity (which is typically 7 m/msec). The f_D resonances have been interpreted by Oya[11] in terms of the instability introduced by Harris[1] together with a nonlinear interaction of the plasma waves associated with the f_D and f_Q sequences of resonances and the $2f_H$ resonance.

In order to illustrate the received signals that are attributed to the Harris instability, two ISIS 1 satellite passes were selected which contained data covering a wide f_N range and a narrow f_H range. This situation is desirable because it allows the spectral changes of a nearly fixed frequency pattern of nf_H resonances to be observed as f_T sweeps through the pattern. The variation of the plasma parameter f_N/f_H for the data of interest is shown in Fig. 3 together with the variation of satellite altitude and the change in dip latitude. (The dip latitude is obtained from the dipole field expression $\tan^{-1}$ (1/2 tan I) when I is set equal to the inclination of the true magnetic field direction from the horizontal.) The

corresponding ionospheric data are presented in Figures 4 and 5. Fig. 4 is a composite presentation of a series of ionograms corresponding to the range of f_N/f_H given in Fig. 3a; similarly, Fig. 5 corresponds to Fig. 3b. Together, the observations illustrate the change in spectral composition of each nf_H resonance between n = 2 and n = 10 as the plasma conditions change from $f_T > nf_H$ to $f_T < nf_H$. The f_T resonance (designated by T in the figures) occurs between the plasma frequency (designated by P) and the exit frequency of the electromagnetic x trace (designated by X); it is not labeled on the ionograms where it is not a prominent feature. The main features to note in Figures 4 and 5 are the following:

(1) The nf_H resonances are observed over a wider frequency range and with a longer time duration when $nf_H < f_T$ than when $nf_H > f_T$.

(2) In the former case, a diffuse signal is observed to extend from nf_H to lower frequencies but not below the mid-point between $(n-1)f_H$ and nf_H.

(3) In general, this diffuse signal appendage is observed to be strongest on the nf_H resonances nearest to, but less than, f_T.

(4) The time duration of the diffuse signal increases as the frequency approaches nf_H.

(5) The nf_H signal is greatly enhanced when the exit frequency of the electromagnetic z trace at the satellite coincides with nf_H.[23]

The first two observational points agree with the theoretical expectations for the Harris instability as outlined in the introduction. The third point may be related to the calculations of Oya[11] which indicate a slight displacement of the instability region to higher kR values for a given anisotropy as f_N/f_H increases. A higher $T_\perp/T_\parallel$ ratio would then be required to produce the instability near nf_H

(low kR value) when $f_T >> nf_H$ than when $f_T \gtrsim nf_H$. One must use caution, however, when interpreting the observations for the dependence of signal strength on f_N/f_H since instrumental effects can be important.[21] The fourth point appears opposite to expectations since the instability growth rate is expected to be greater for the frequency range near the midpoint between the nf_H values rather than near nf_H (see Fig. 1). The capability of generating the required anisotropy must also be considered and, in the next section, it will be shown that the anisotropy produced by the transmitter is much greater near nf_H. Also, the finite antenna size may play a fundamental role in determining the spectral response since the wavelength of the oscillations increases as the frequency approaches nf_H. The fifth point implies that more energy can be fed into the electrostatic mode when it coincides in frequency with the electromagnetic cutoff of the z trace. This observation has been noted earlier[17].

DISCUSSION

The main question pertaining to the interpretation of the present observations in terms of the Harris instability concerns the generation of the required electron temperature anisotropy. The anisotropy required for the instability near nf_H is given by[8]

$$T_\perp/T_\parallel > 2n. \tag{1}$$

Large anisotropies of this type can be created by the rf electric field of the sounder pulse since more energy is absorbed by the component of electron motion perpendicular to $\vec{B}$ than by the component parallel to $\vec{B}$ due to the collisionless cyclotron damping process. The magnitude of this damping is illustrated in Fig. 6. The absorption is very severe and it increases as the propagation angle θ decreases (cyclotron damping is not present for propagation perpendicular to $\vec{B}$, i.e., when $\theta = 90°$). The figure corresponds to $k_\perp R$ fixed and θ variable, θ decreases as the frequency approaches the value of $2f_H$. This behavior is illustrated very vividly by the calculations of Oya[11] which show that the dispersion curves are much closer to the nf_H frequency value when $\theta << 90°$ than when $\theta = 90°$ for the condition of interest, i.e., $f_T > nf_H$. Thus the cyclotron damping of plasma waves is much greater near the harmonics of f_H than it is in the frequency region mid way between the harmonics. This increased cyclotron damping near nf_H could explain the increased signal strength observed near nf_H (as pointed out in item 4 of the last section), since the amount of transmitted energy absorbed by the medium increases dramatically as the sounder frequency approaches nf_H. The result of this energy absorption will be to increase $T_\perp$ in the region around the sounder antenna.

In order to estimate whether this increase in $T_\perp$ is significant with respect to the thermal electron energy, it is necessary to know the effective plasma volume for energy absorption and the energy of the transmitted wave. The magnitude of the absorption indicated in Fig. 6 (i.e., 10's of dB per cyclotron period) suggests that the effective volume of enhanced $T_\perp$, due to the absorption of plasma waves propagating with low group velocity, is very small.

Observations[17] indicate that the signals responsible for the higher order nf_H resonances have near zero group velocity and that they do not extend beyond about two meters in the radial direction from the antenna element. These conclusions were based on the nf_H resonances excited when $nf_H > f_T$, i.e., when the instability condition is not satisfied. The present observations indicate that the nf_H resonances persist for a longer time duration when $nf_H < f_T$ due to the Harris instability. If, however, it is assumed that the instability region extends over a region of space of the same order of magnitude in size as the region covered by the plasma waves when no instability is present, then an estimate of the energy density absorbed from the rf sounder pulse can be made. Next, it is necessary to make an estimate of the fraction of the transmitted energy that will be available in the electrostatic mode (which will be the effective mode for energy absorption in the region near the antenna). It is apparent from the regular reception of ionospheric echoes over distances of the order of thousands of kilometers (e.g., see Figures 4 & 5) that a very significant amount of energy is radiated in the electromagnetic mode. It is also apparent from the intensity of the plasma resonance signals (again - see Figures 4 & 5) that a very significant amount of energy is radiated in the electrostatic mode. (Evidence for significant energy radiation in the form of electrostatic waves from an antenna immersed in the ionospheric plasma is also available from in situ impedance measurements - as first pointed out by Whale[25]). For the sake of discussion, assume that 1/2 of the total energy contained in the sounder pulse is available in the electrostatic mode and that this energy is absorbed in a cylindrical volume extending a radial distance r from the antenna of tip-to-tip length L. Then the absorbed energy

density is $(P/2)\tau/(\pi r^2 L)$ where the ISIS 1 sounder power P and pulse length τ are 400 w and 98 μsec, respectively. When r = 2m and L = 73m (for the long dipole antenna), the absorbed energy density is 2×10^{-4} ergs/cm^3 which is more than 3 orders of magnitude larger than the thermal energy density of 10^{-7} ergs/cm^3 based on $N = 3.6 \times 10^5$ cm^{-3} and T = 2000°K (as appropriate for the data of Figure 4d). Such a large value for the energy absorption indicates that the estimates for the fraction of transmitted power and for the size of the absorption region have considerable leeway while the instability anisotropy requirement of (1) remains satisfied.

The above estimate of a few meters for the region of enhanced $T_\perp/T_\parallel$ is comparable to the distance covered by the wave packet propagating in the electrostatic mode during a time interval equal to the sounder pulse duration[26]. This time interval is equal to about 60 times the electron cyclotron period and the results of Fig. 6 indicate that waves propagating at oblique angles with $\theta \ll 90°$ would be completely damped out in a much shorter time. The calculations leading to Fig. 6, however, are appropriate only for a particular value of $k_\perp R$ (namely $k_\perp R = 1.0$) and for an isotropic plasma. When smaller $k_\perp R$ values are considered, then the dispersion curves corresponding to $\theta \lesssim 90°$ (where the least cyclotron damping occurs) approach the frequency at nf_H[11]. Also, in an anisotropic plasma with $T_\perp/T_\parallel > 1$ the cyclotron damping is reduced as can be seen by writing the condition for negligible cyclotron damping[27]

$$\left| \frac{\omega + n\omega_H}{k_\parallel} \left(\frac{m}{2\kappa T_\parallel} \right)^{1/2} \right| >> 1$$

in the form:

$$k_{\parallel} R << \left(\frac{T_{\perp}/T_{\parallel}}{2}\right)^{1/2} \left|\frac{\omega}{\omega_H} - n\right| \qquad (2)$$

where κ is Boltzmann's constant, $\omega = 2\pi f$, $\omega_H = 2\pi f_H$, and $R = (\kappa T_{\perp}/m)^{1/2} \omega_H^{-1}$ is the cyclotron radius. Using (2), and the dispersion equation solutions for $T_{\perp}/T_{\parallel} = 1$ and $T_{\perp}/T_{\parallel} = 10$ as given in Figures 6 and 8b of Oya[11], it can be shown that the range of propagation angles satisfying the condition of negligible cyclotron damping increases with increasing $T_{\perp}/T_{\parallel}$. This result indicates that as energy is absorbed from the leading portion of the rf pulse, an anisotropy is produced which decreases the cyclotron damping for the later portions of the pulse which can then propagate further into the medium. This reduction of cyclotron damping with an increase in $T_{\perp}/T_{\parallel}$ is not very strong, however, because of the power of 1/2 in (2). Thus the figure of a few meters for the extent of the region of large $T_{\perp}/T_{\parallel}$ is a reasonable upper limit, especially near nf_H where the damping is extreme for certain combinations of $k_{\perp} R$ and θ.

The above discussion suggests that the temperature anisotropies required to produce the Harris instability could be produced by the cyclotron damping of electrostatic cyclotron harmonic waves in the vicinity of the sounder antenna, i.e., within a radial distance of a few meters from the antenna element for the higher order harmonics of f_H. It should be noted that this distance is well outside the antenna sheath region which is of the order of a few centimeters. The diffuse signals associated with the nf_H resonances (when $nf_H < f_T$) in Figures 4 and 5 are attributed to this instability.

ACKNOWLEDGMENTS

The data used in this analysis were provided by the National Space Science Data Center at the Goddard Space Flight Center. I am grateful to Mr. D. Verven for his assistance in the data search and to Dr. H. Oya for his helpful correspondence. I am also grateful to Mr. J. E. Jackson and to Drs. S. J. Bauer and R. E. Hartle for helpful discussions.

REFERENCES AND FOOTNOTES

1. E. G. Harris, Phys. Rev. Letters, 2, 34 (1959).
2. See the review article by E. G. Harris in Physics of Hot Plasmas, edited by B. J. Rye and J. C. Taylor (Oliver and Boyd, Edinburgh, 1970) p. 145.
3. See the review article by A. V. Timofee and V. I. Pistunovich in Reviews of Plasma Physics, vol. 5, edited by M. A. Leontovich (Consultants Bureau, New York, 1970) p. 401.
4. See the references given in the review article by B. Lehnert, Plasma Phys. 9, 301 (1967).
5. C. B. Wharton, T. H. Jensen and F. R. Scott, Proceedings of the International Symposium on Properties and Applications of low temperature plasma at the 20th International Congress on Pure and Applied Chemistry, Moscow, 15-17 July 1965, edited by a commission headed by A. E. Scheindlin ("MIR" Publishing House Moscow, 1967) p. 111.
6. L. S. Hall, W. Heckrotte, and T. Kammash, Phys. Rev. 139, A1117 (1965).
7. M. J. Schwartz and A. J. Lichtenberg, Phys. Fluids 15, 470 (1972).
8. E. G. Harris, General Atomic Report No. 5581 (1964).
9. Y. Shima and L. S. Hall, Phys. Rev. 139, A1115 (1965).
10. S. Gruber, M. W. Klein, and P. L. Auer, Phys. Fluids 8, 1504 (1965).
11. H. Oya, Phys. Fluids 14, 2487 (1971).

12. See the Special Issue on Topside Sounding and the Ionosphere: Proc. IEEE 57, 859 (1969). See also the ISIS 2 results of G. G. Shepherd, C. D. Anger, L. H. Brace, J. R. Burrows, W. J. Heikkila, J. Hoffman, E. J. Maier, and J. H. Whitteker, Planet. Space Sci. 21, 819 (1973).

13. J. R. McAfee, J. Geophys. Res. 73, 5577 (1968); J. R. McAfee, J. Geophys. Res. 74, 6403 (1969); see also the following papers and references therein: P. Graff, J. Geophys. Res. 76, 1060 (1971); P. Graff, J. Plasma Phys. 5, 427 (1971).

14. J. M. Warnock, J. R. McAfee, and T. L. Thompson, J. Geophys. Res. 75, 7272 (1970); R. F. Benson, J. Geophys. Res. 76, 1083 (1971); R. Feldstein and P. Graff, J. Geophys. Res. 77, 1896 (1972); J. R. McAfee, T. L. Thompson, W. Calvert, and J. M. Warnock, J. Geophys. Res. 77, 5542 (1972).

15. M. K. Andrews and M. T. C. Fang, J. Plasma Phys. 6, 579 (1971).

16. D. B. Muldrew, Radio Sci. 7, 779 (1972).

17. R. F. Benson, Planet Space Sci. 20, 683 (1972).

18. E. S. Warren and E. L. Hagg, Nature 220, 466 (1968).

19. H. Oya, J. Geophys. Res. 75, 4279 (1970).

20. D. B. Muldrew, J. Geophys. Res. 77, 1794 (1972).

21. The ISIS 2 satellite uses an orthogonal pair of dipole antennas to cover the desired frequency range. The crossover frequency between antennas occurs at 5 MHz. Thus signals received at frequencies considerably

above 5 MHz are received on an antenna which is perpendicular to the antenna of importance when the frequency is considerably less than 5 MHz.

22. The frequency sweep rate is significantly non-linear in the frequency ranges 2.0 MHz to 3.0 MHz and 5.0 MHz to 6.0 MHz.

23. The exit frequency of the f_Z trace is not labeled on the ionograms where it is not a prominent feature; it can be calculated from the observed exit frequency of the f_X trace and f_H using the expression $f_Z = f_X - f_H$.

24. J. A. Tataronis and F. W. Crawford, J. Plasma Phys. 4, 249 (1970).

25. H. A. Whale, J. Geophys. Res. 68, 415 (1963).

26. The group velocity for the electrostatic waves is of the order of 100 m/msec and the pulse duration is 0.1 msec. Thus the leading edge of the wave packet would have attained a distance of the order of 10 m from the sounder antenna at the time of the sounder pulse termination.

27. T. H. Stix, The Theory of Plasma Waves (McGraw-Hill, New York, 1962) p. 226.

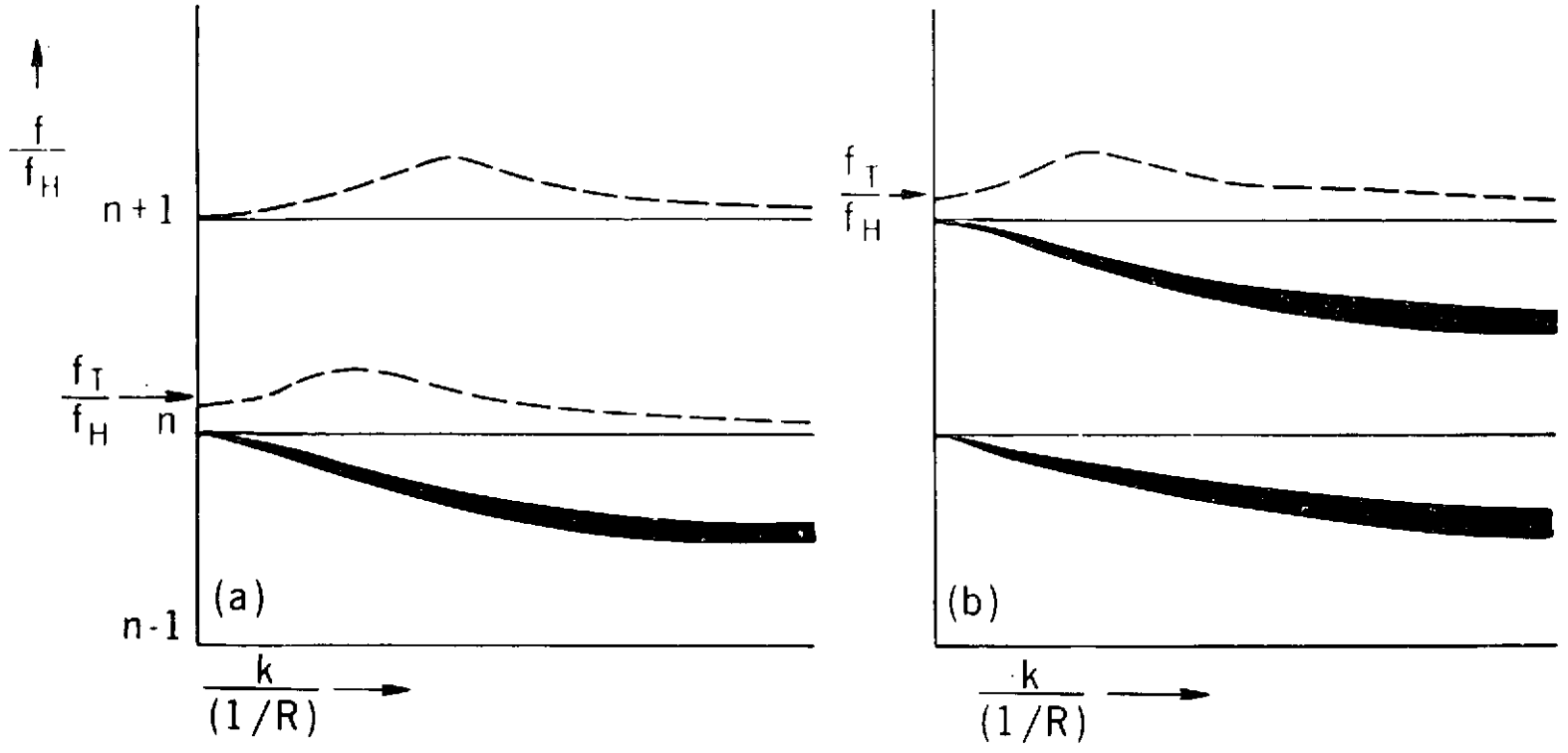

Figure 1. Schematic normalized dispersion curves for the electron electrostatic cyclotron harmonic waves. The dashed curves correspond to waves that are not subject to the Harris instability whereas the solid curves are subject to this instability if the required electron temperature anisotropy is present. The increasing thickness of the solid curves indicates the increasing instability growth rate with increasing wave number (decreasing wavelength). Note the change in the location of the dispersion curve associated with $(n + 1)\, f_H$ from the stable region above $(n + 1)\, f_H$ when $f_T < (n + 1)\, f_H$ in (a) to the unstable region below $(n + 1)\, f_T$ when $f_T > (n + 1)\, f_H$ in (b).

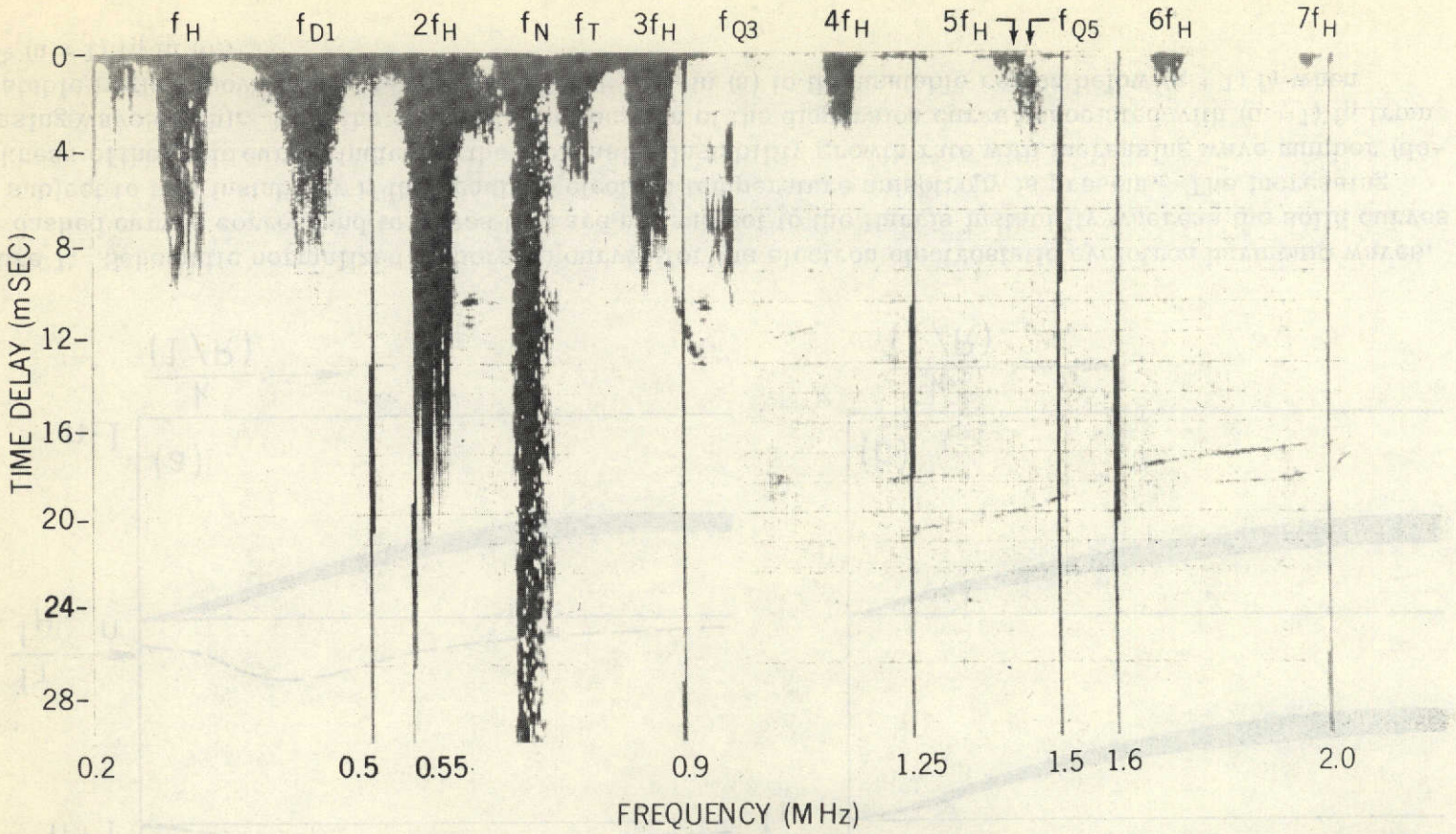

Figure 2. The high resolution portion of an Alouette 2 ionogram recorded at the Quito Telemetry Station on 4 May 1967 (12:14:22 UT; 25.2°S, 65.8°W, 2612 km in altitude). The heavy vertical lines are frequency markers and the horizontal lines are range markers separated by 200 km in range or 4/3 msec of delay time. The heavy vertical traces, which are due to electrostatic waves of low group velocity in the vicinity of the sounder, are identified at the top of the ionogram; the weaker non vertical traces are due to the ionospheric reflection of electromagnetic waves radiated by the sounder.

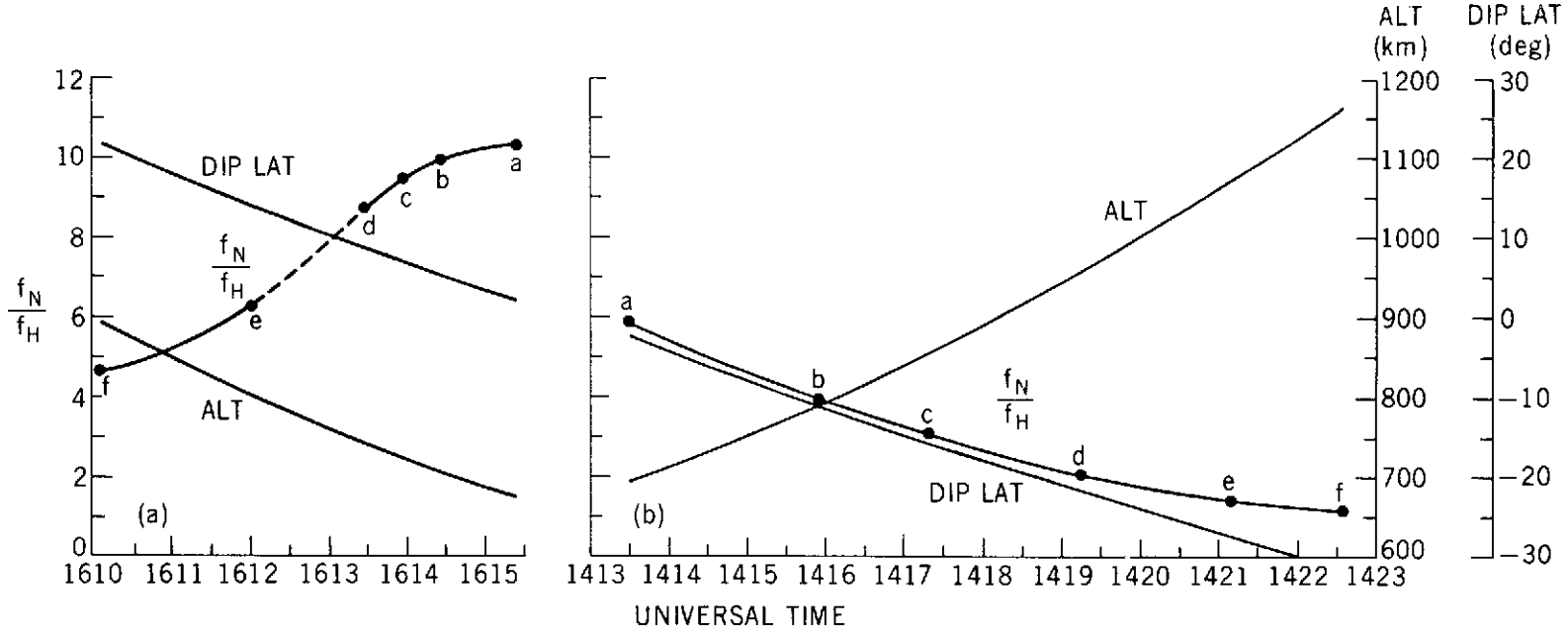

Figure 3. The variation of the ambient plasma parameter f_N/f_H, the ISIS 1 altitude, and the dip latitude as a function of universal time for (a) QUI pass 1776 on 7 July 1969 and (b) SNT pass 2033 on 30 July 1969. The letters a-f on the f_N/f_H curves correspond to the ionogram data presented in Figures 4 and 5. (The dashed portion of the f_N/f_H curve in (a) corresponds to a period of missing data due to interference.)

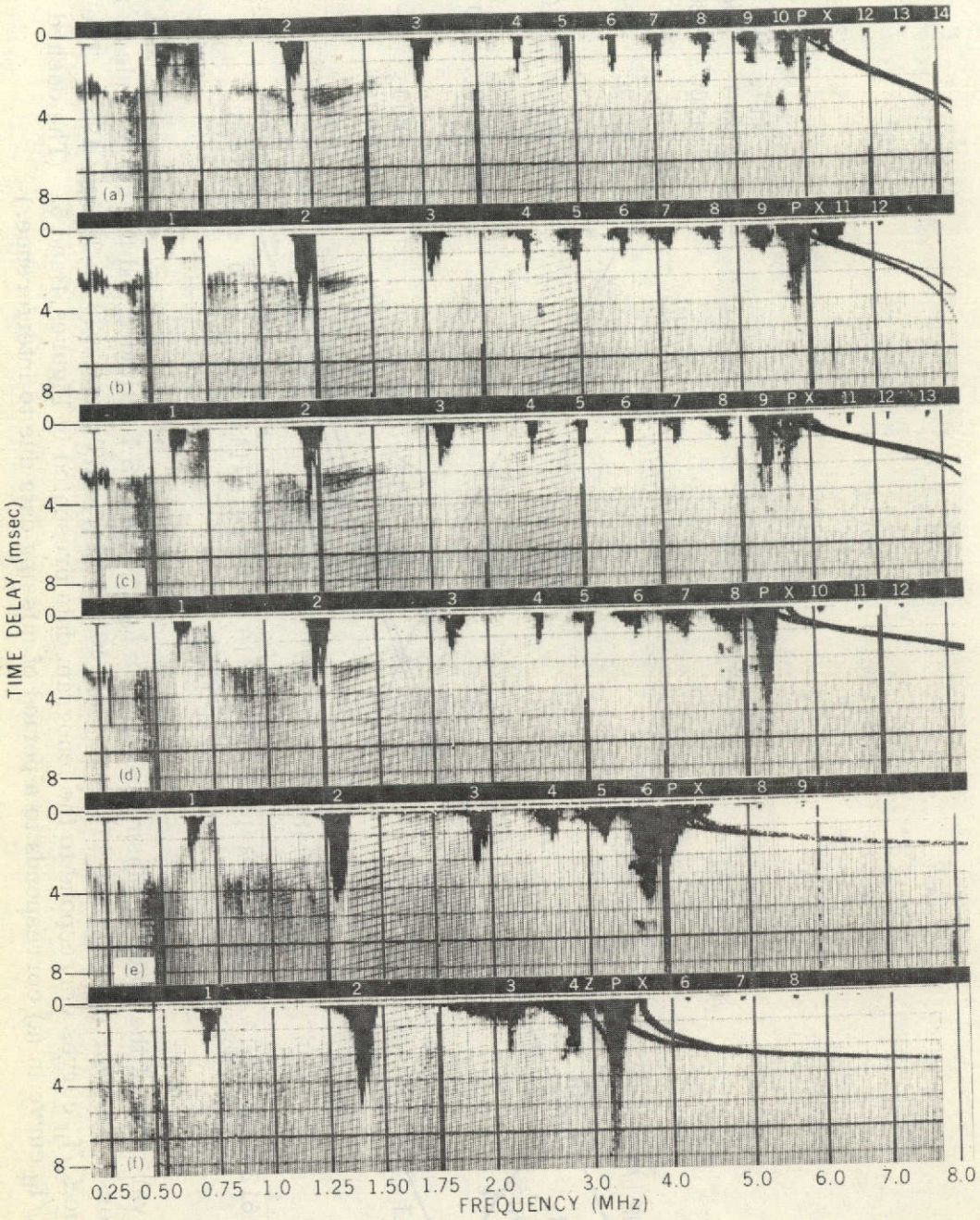

Figure 4. A series of ISIS 1 ionograms from QUI pass 1776 corresponding to the conditions given in Figure 3a. The letters 1 through 14 are used to identify the resonances at f_H through 14 f_H, P represents the plasma frequency resonance at f_N, Z and X represent the cut-off frequency at the satellite for the electromagnetic z and x traces, respectively. Certain instrumental effects[21, 22] must be considered when evaluating these ionograms.

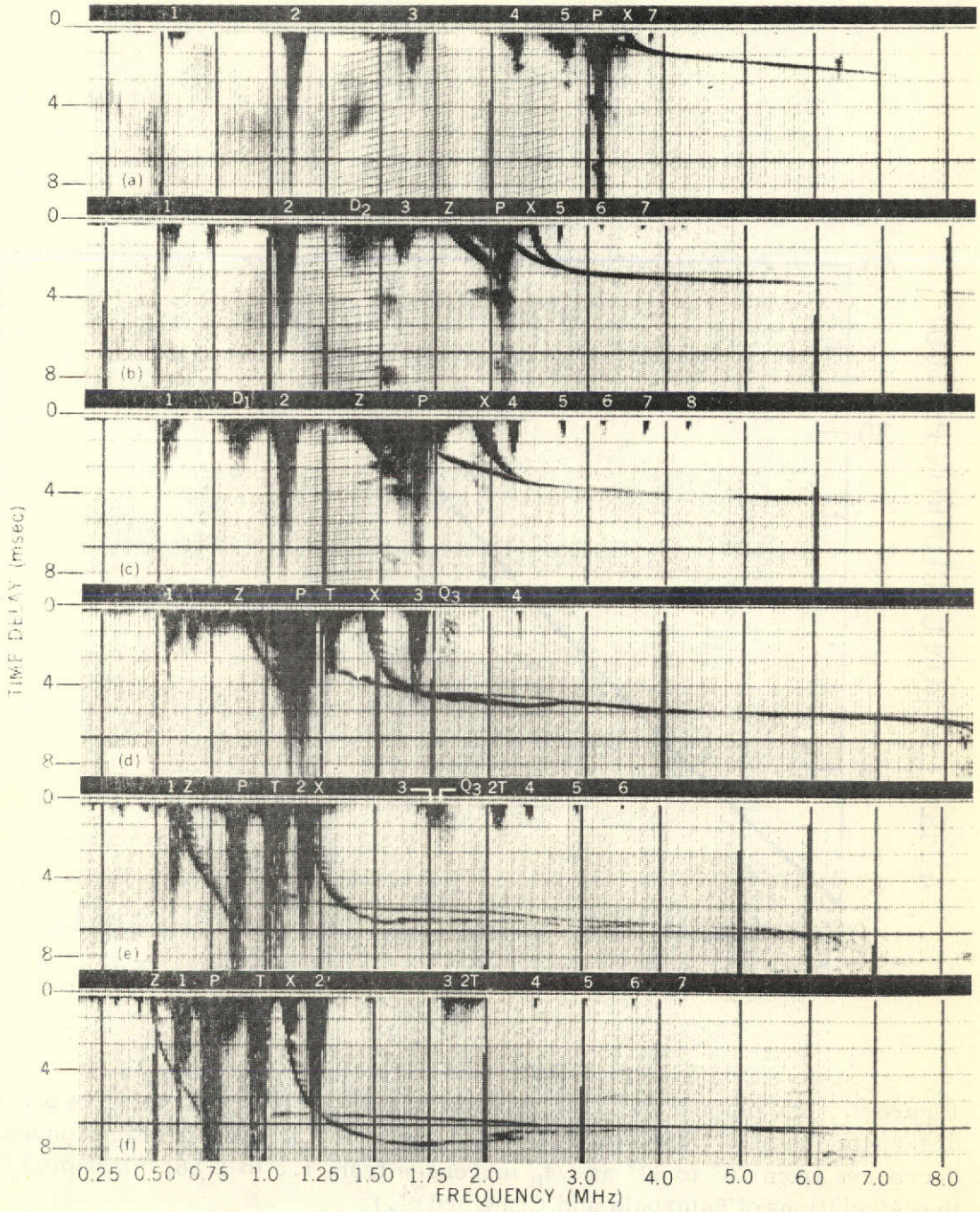

Figure 5. A series of ISIS 1 ionograms from SNT pass 2033 corresponding to the conditions given in Figure 3b. D_1 and D_2 represent the diffuse resonances at f_{D1} and f_{D2}, respectively. Q_3 represents the electrostatic resonance at f_{Q3} and T represents the upper hybrid resonances at f_T.

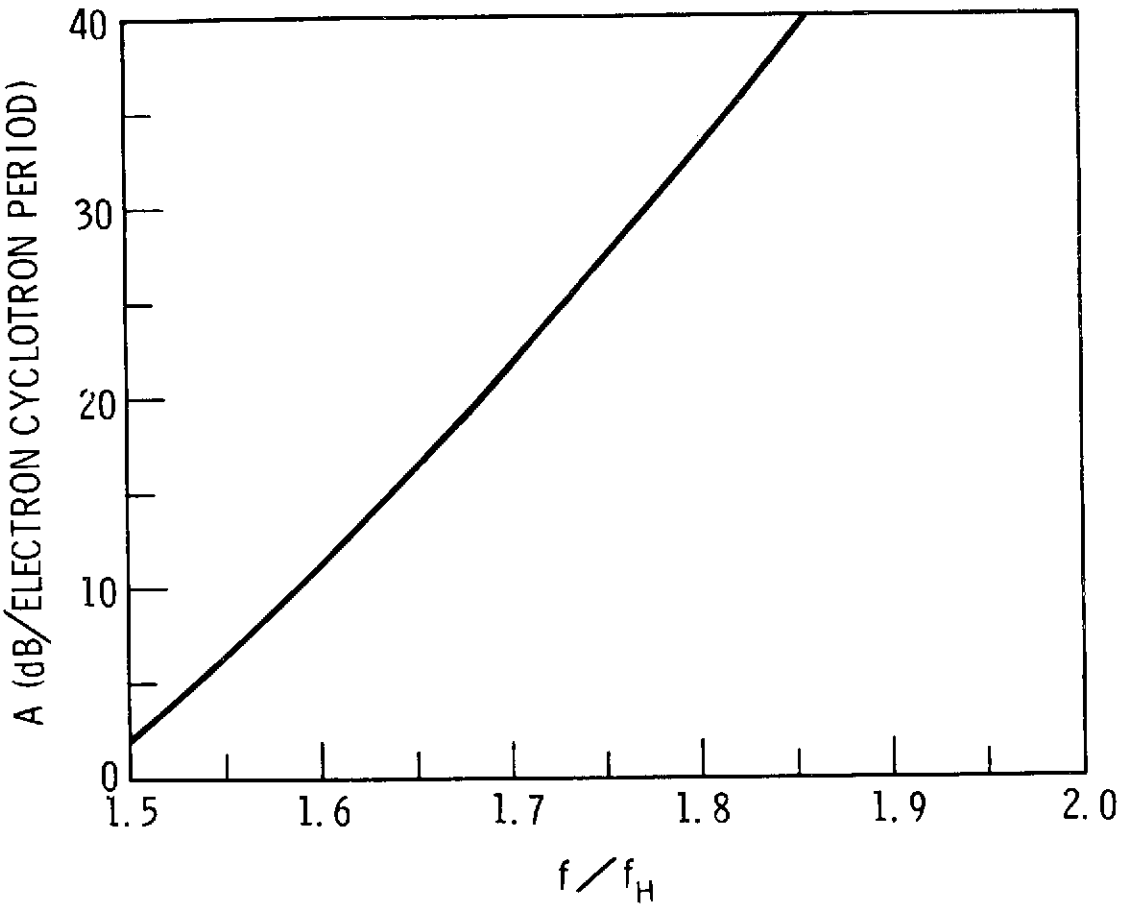

Figure 6. The plasma wave absorption A due to cyclotron damping as a function of f/f_H for the case where $(f_N/f_H)^2 = 5.0$ and $k_\perp R = 1.0$ (the propagation angle decreases from 79° to 63° as f/f_H increases from 1.5 to 1.86). (Adapted from the calculations of Tataronis and Crawford [24].)